Journal of Catalysis 259 (2008) 133–137

Contents lists available at ScienceDirect

Journal of Catalysis

www.elsevier.com/locate/jcat

The effect of co-catalyst for Z-scheme photocatalysis systems with an Fe^{3+}/Fe^{2+} electron mediator on overall water splitting under visible light irradiation

Yasuyoshi Sasaki [a], Akihide Iwase [a], Hideki Kato [a,1], Akihiko Kudo [a,b,*]

[a] Department of Applied Chemistry, Faculty of Science, Tokyo University of Science, 1-3 Kagurazaka, Shinjuku-ku, Tokyo 162-8601, Japan
[b] Core Research for Evolutional Science and Technology, Japan Science Technology Agency (CREST/JST), Japan

ARTICLE INFO

Article history:
Received 2 May 2008
Revised 23 June 2008
Accepted 31 July 2008
Available online 23 August 2008

Keywords:
Heterogeneous photocatalysis
Water splitting
Solar hydrogen
Visible light
Z-scheme
Co-catalyst
Ruthenium

ABSTRACT

Co-catalysts loaded on $SrTiO_3$:Rh in visible-light-driven Z-scheme photocatalysis systems consisting of $SrTiO_3$:Rh for H_2 evolution, $BiVO_4$ for O_2 evolution, and Fe^{3+}/Fe^{2+} for an electron mediator were investigated. The activity of the system using a Ru co-catalyst for overall water splitting was as high as that of the system using a Pt co-catalyst. The photocatalytic activity of the system using the Pt co-catalyst decreased as the partial pressures of evolved H_2 and O_2 were increased. In contrast, such deactivation was not observed for the system using the Ru co-catalyst. The investigation of the back-reactions revealed that water formation from H_2 and O_2, reduction of Fe^{3+} by H_2, and oxidation of Fe^{2+} by O_2 were significantly suppressed in the system using the Ru co-catalyst, resulting in good photocatalytic performance for water splitting. The (Ru/$SrTiO_3$:Rh)–($BiVO_4$)–(Fe^{3+}/Fe^{2+}) photocatalysis system gave a quantum yield of 0.3% and a stable activity more than 70 h. This system was confirmed to be active for water splitting using a solar simulator.

1. Introduction

Photocatalytic overall water splitting has been studied as a potential technique for H_2 production by photon energy conversion. There are many reports of overall water splitting under UV irradiation using powdered photocatalysts [1–12]; however, it is important to develop visible-light-driven photocatalysts in terms of solar energy use. Metal oxide [13–17], metal (oxy)sulfide [18–20], and metal (oxy)nitride [21,22] photocatalysts have been reported to produce H_2 or O_2 from aqueous solutions containing sacrificial reagents under visible light irradiation. In contrast, photocatalytic overall water splitting under visible light irradiation on a single photocatalyst has been limited. Domen and co-workers have reported overall water splitting under visible light irradiation using oxynitride GaN–ZnO and $GeZnN_2$–ZnO solid solution photocatalysts [23–25]. These oxynitride photocatalysts are not active without assistance of co-catalysts; however, these photocatalysts showed activity when Cr_2O_3–Rh_2O_3 co-catalysts were loaded. Thus, co-catalysts play an important role in photocatalytic reactions for water splitting and H_2 or O_2 evolution from aqueous solutions [2,4,7,26–33]. Therefore, the development of a co-catalyst is important for photocatalysis research.

Overall water splitting using a two-step photoexcitation systems (Z-scheme) mimicking photosynthesis in a green plant also has been studied. The Z-scheme photocatalysis system is composed of two photocatalysts for H_2 and O_2 evolution, along with a reversible redox couple. The redox couple plays a role in electron transfer from the O_2 production photocatalyst to the H_2 production photocatalyst (designated O_2- and H_2-photocatalysts). Fujihara et al. achieved overall water splitting using a system consisting of Pt/TiO_2-Br^- and TiO_2-Fe^{3+} components, but this system worked only under UV light irradiation [34]. Some visible-light responsive systems have been reported [35–37]. Sayama et al. and Abe et al. constructed visible-light-driven Z-scheme photocatalysis systems using an IO_3^-/I^- redox couple as an electron mediator [35,36]. We also found visible-light-driven Z-scheme photocatalysis systems composed of Pt/$SrTiO_3$:Rh [15] for a H_2-photocatalyst, $BiVO_4$ [14], Bi_2MoO_6 [16], and WO_3 [13] for O_2-photocatalysts, and an Fe^{3+}/Fe^{2+} electron mediator, as shown in Fig. 1 [37,38]. In these systems, overall water splitting proceeds despite the suspension system using a Pt co-catalyst on which back-reactions, such as water formation, from evolved H_2 and O_2 proceed readily. The back-reactions are suppressed by adsorption of Fe^{3+} ions on the Pt co-catalyst. But when the pressures of H_2 and O_2 evolved become high, the back-reactions cannot be neglected. Therefore, it is important to find a suitable co-catalyst for H_2 evolution besides

* Corresponding author at: Department of Applied Chemistry, Faculty of Science, Tokyo University of Science, 1-3 Kagurazaka, Shinjuku-ku, Tokyo 162-8601, Japan. Fax: +81 3 5261 4631.
E-mail address: a-kudo@rs.kagu.tus.ac.jp (A. Kudo).
[1] Present address: Materials and Structures Laboratory, Tokyo Institute of Technology, Japan.

0021-9517/$ – see front matter
doi:10.1016/j.jcat.2008.07.017

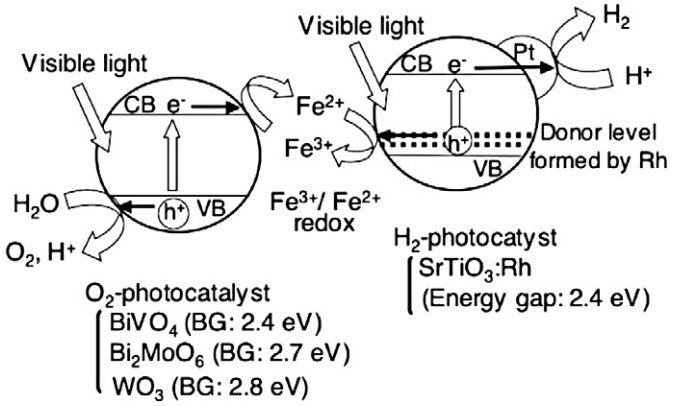

Fig. 1. Mechanism of overall water splitting using a Z-scheme photocatalysis system.

Pt, to improve the photocatalytic performance of the Z-scheme systems.

In the present work, highly efficient co-catalysts for H_2 evolution in the present Z-scheme photocatalysis systems using an Fe^{3+}/Fe^{2+} electron mediator were studied. Solar hydrogen production from water was demonstrated using the optimized photocatalysis system.

2. Experimental

Rh-doped (1 atom%) $SrTiO_3$ (designated $SrTiO_3$:Rh) and $BiVO_4$ powders were prepared as described previously [14,15]. Commercial WO_3 powder (Nacalai Tesque; 99.5%) was used as received. X-ray diffraction (Rigaku; MiniFlex) confirmed that the obtained powder had a single phase. Various co-catalysts were loaded on $SrTiO_3$:Rh by photodeposition and impregnation. Ni (0.3 wt%), Ru (0.3–1 wt%), Rh (0.3 wt%), Ag (0.3 wt%), and Pt (0.1–0.3 wt%) co-catalysts were loaded by photodeposition in Ar gas at 40 Torr pressure and 293 K from aqueous methanol solutions of $Ni(NO_3)_2{\cdot}6H_2O$ (Wako Pure Chemical; 98.0%), $RuCl_3{\cdot}nH_2O$ (Wako Pure Chemical; 99.9%), $RhCl_3{\cdot}3H_2O$ (Tanaka Kikinzoku; 36% as Rh), $AgNO_3$ (Tanaka Kikinzoku; 99.8%), and H_2PtCl_6 (Tanaka Kikinzoku; 37.55% as Pt). The co-catalyst-loaded photocatalysts were collected by filtration, washed with water, and then dried at room temperature in air. Au (0.3 wt%), Fe_2O_3 (0.3 wt%), NiO (0.3 wt%), and RuO_2 (0.3 wt%) co-catalysts were loaded on $SrTiO_3$:Rh by impregnation. $SrTiO_3$:Rh powder was immersed in aqueous solutions of $HAuCl_4{\cdot}4H_2O$ (Kanto Chemical; 99.0%), $Fe(NO_3)_3{\cdot}9H_2O$ (Kanto Chemical; 99.0%), and $Ni(NO_3)_2{\cdot}6H_2O$ (Wako Pure Chemical; 98.0%) for deposition of Au, Fe_2O_3, and NiO co-catalysts respectively. An acetone solution of $Ru_3(CO)_{12}$ (Aldrich; 99%) also was used for RuO_2 deposition [7]. After drying, the powders were annealed with various conditions: at 423 K for 1 h with H_2 for Au, at 543 K for 1 h in air for Fe_2O_3, at 543 K for 1 h in air for NiO, and at 673 K for 1 h in air for RuO_2. Pretreatment of H_2 reduction at 773 K for 2 h at 200 Torr, followed by oxidation at 473 K for 1 h at 100 Torr, was conducted for a NiO-loaded photocatalyst to form NiO_x with an effective core–shell structure [4]. The powder was observed by scanning electron microscopy (JEOL; JSM-7400F). The surfaces of loaded co-catalysts were investigated by X-ray photoelectron spectroscopy (KRATOS; ESCA-3400).

Photocatalytic reactions were conducted in a gas closed-circulation system and an Ar flow system. Photocatalyst powders (50 mg) were dispersed in an aqueous $FeCl_3$ solution (120 mL) by a magnetic stirrer in a Pyrex reaction cell. The reactant solution was adjusted to pH 2.4 with H_2SO_4 and maintained at 293 K. The photocatalysts were irradiated with visible light ($\lambda > 420$ nm) through a cutoff filter (HOYA; L42) from a 300-W Xe-arc lamp (Perkin Elmer; Cermax-PE300BF). A solar simulator with an air mass 1.5 filter (Yamashita denso; YSS-80QA) also was used. The amounts of evolved H_2 and O_2 were determined by online gas chromatography (Shimadzu; GC-8A, MS-5A column, TCD, Ar carrier).

Table 1
Effect of co-catalysts on water splitting by ($SrTiO_3$:Rh)–(WO_3) systems

Co-catalyst	Loading method	Amounts of products for 22 h (μmol)[a]	
		H_2	O_2
None	–	21	51
Ni	Photodeposition	60	42
Ru	Photodeposition	416	197
Rh	Photodeposition	92	67
Ag	Photodeposition	7.1	39
Pt	Photodeposition	322	153
Au	Impregnation	140	71
Fe_2O_3	Impregnation	15	55
NiO_x	Impregnation	0.9	33
RuO_2	Impregnation	4.4	38

[a] Reaction conditions: catalyst, 50 mg each; reactant solution, 2 mmol L^{-1} of an aqueous $FeCl_3$ solution; 120 mL; pH 2.4; light source, 300-W Xe-arc lamp ($\lambda > 420$ nm); cell, top-irradiation cell with a Pyrex glass window.

Back-reactions, such as water formation and the reduction of Fe^{3+} ions by H_2, were examined in the presence of photocatalyst powders (50 mg) in an aqueous $FeCl_3$ solution adjusted to pH 2.4 with H_2SO_4 in the dark. After introduction of 20 Torr of a H_2 gas and 10 Torr of an O_2 gas into the reaction system, the decreases in gas pressures were monitored. Oxidation of Fe^{2+} ions also was evaluated in the presence of photocatalyst powders (100 mg) in an aqueous $FeCl_2$ solution adjusted to pH 2.4 with H_2SO_4 in air in the dark. The concentrations of Fe^{2+} and Fe^{3+} ions for 3 h were determined by colorimetric analysis based on 1,10-phenanthrorine–iron(II) complex [38].

A turnover number was defined by the following equation:

$$\text{Turnover number} = [\text{the number of reacted electrons}] / [\text{the total number of Ru loaded on } SrTiO_3\text{:Rh}].$$

Apparent quantum yields defined by the following equation were measured using filters combined with bandpass (Kenko) and cutoff filters and a photodiode (OPHIRA; PD300-UV of a head and NOVA of a power monitor). In the Z-scheme system, H_2 is produced by a four-electron process:

$$\text{Apparent quantum yield (\%)} = [\text{the number of reacted electrons}] / [\text{the number of incident photons}] \times 100 = [\text{the number of evolved } H_2 \text{ molecules} \times 4] / [\text{the number of incident photons}] \times 100.$$

3. Results and discussion

3.1. Overall water splitting by Z-scheme photocatalysis system, ($SrTiO_3$:Rh)–(WO_3), using various co-catalysts

Table 1 presents the activities of Z-scheme photocatalysis systems consisting of $SrTiO_3$:Rh loaded with various co-catalysts and WO_3 for overall water splitting. Loading Ni, Ru, Rh, Pt, and Au co-catalysts on $SrTiO_3$:Rh enhanced water splitting compared with that in a nonloaded system, due to increased H_2 production. The system using a photodeposited Ru co-catalyst exhibited high photocatalytic performance, as did the system using a Pt co-catalyst. Au has been reported to work as a co-catalyst for overall water splitting [32] and H_2 evolution from an aqueous ethanol solution [27]. Au also was effective in the present system. The ratios of evolved H_2 to O_2 deviated from stoichiometry when H_2 production

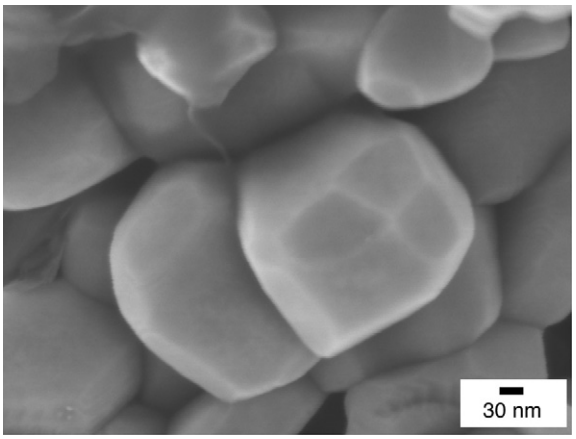

(a)

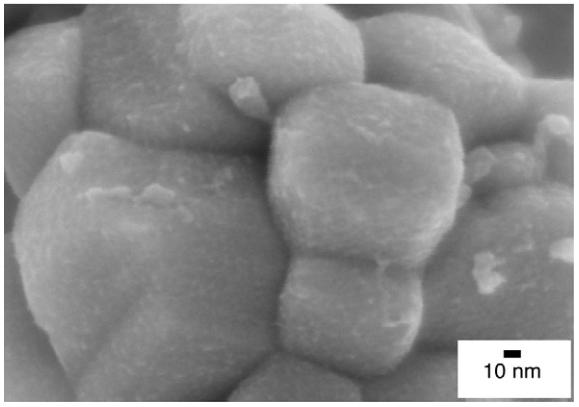

(b)

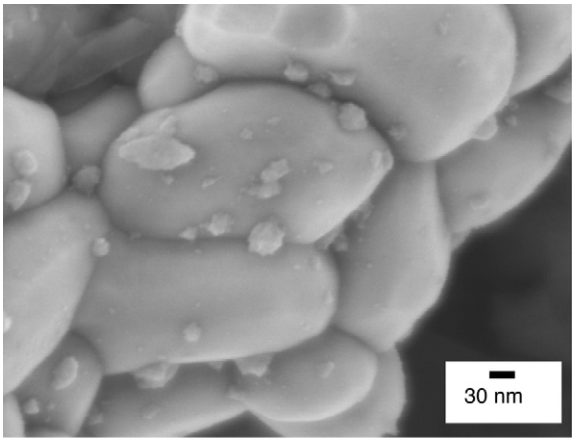

(c)

Fig. 2. Scanning electron microscope images of (a) naked $SrTiO_3$:Rh, (b) 0.7 wt% of Ru loaded by photodeposition, and (c) 0.3 wt% of RuO_2 loaded by impregnation on $SrTiO_3$:Rh photocatalyst.

was poor, due to dominant O_2 production on the WO_3 photocatalyst at the initial stage of the reaction using an aqueous $FeCl_3$ solution [38].

There have been some reports that metallic Ru functions more efficiently that Pt as a co-catalyst for water splitting [2] and H_2 production in the presence of electron donors [29,30]. A RuO_2 co-catalyst has been used for overall water splitting [7,25,26]. The Ru co-catalyst formed after photodeposition was effective, whereas that loaded by an impregnation method was not effective in the present Z-scheme system, as shown in Table 1. Because the effect of the RuO_2 co-catalyst depends strongly on the condition of the RuO_2, we investigated the difference in condition between

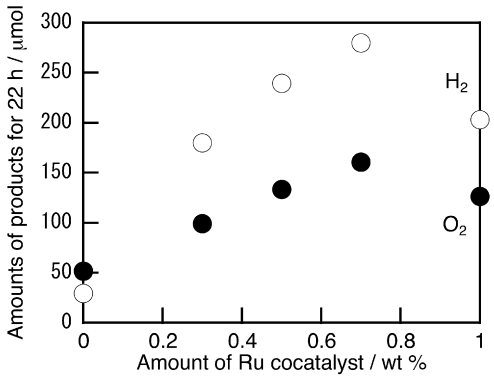

Fig. 3. Dependence of the activity of the (Ru/$SrTiO_3$:Rh)–($BiVO_4$)–($FeCl_3$) system upon the amount of Ru co-catalyst loaded on $SrTiO_3$:Rh. Catalyst: 50 mg each, reactant solution: 2 mmol L^{-1} of aqueous $FeCl_3$ solution, 120 mL, pH 2.4, light source: 300-W Xe-arc lamp ($\lambda > 420$ nm), cell: top-irradiation cell with a Pyrex glass window.

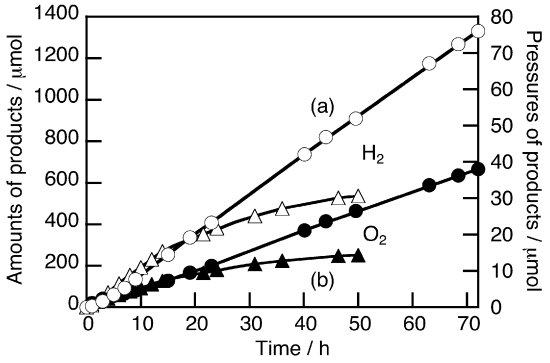

Fig. 4. Photocatalytic overall water splitting on (a) the (Ru (0.7 wt%)/$SrTiO_3$:Rh)–($BiVO_4$) system and (b) the (Pt (0.1 wt%)/$SrTiO_3$:Rh)–($BiVO_4$) system. Catalyst: 50 mg each, reactant solution: 2 mmol L^{-1} of aqueous $FeCl_3$ solution, 120 mL, pH 2.4, light source: 300-W Xe-arc lamp ($\lambda > 420$ nm), cell: top-irradiation cell with a Pyrex glass window.

photodeposited Ru and impregnated RuO_2 co-catalysts by XPS and SEM. XPS analyses indicated that the surface of Ru loaded by photodeposition was oxidized by air or water. Fig. 2 shows SEM images of the Ru co-catalysts loaded by photodeposition and RuO_2 co-catalysts loaded by impregnation on $SrTiO_3$:Rh. The photodeposited Ru particles, ranging in size from 1 to 5 nm, were highly dispersed and well attached on the $SrTiO_3$:Rh support. In contrast, RuO_2 particles loaded by impregnation were poorly dispersed. This difference in the condition of the loaded RuO_2 co-catalyst accounts for the difference in catalytic performance.

3.2. Overall water splitting by a (Ru/$SrTiO_3$:Rh)–($BiVO_4$) system using an Fe^{3+}/Fe^{2+} electron mediator

Fig. 3 shows the dependence of the photocatalytic activity of the (Ru/$SrTiO_3$:Rh)–($BiVO_4$)–($FeCl_3$) system for overall water splitting on the amount of Ru co-catalyst loaded. The highest activity was obtained when 0.7 wt% of Ru was loaded. Co-catalysts loaded on photocatalysts provide not only active sites, but also a shielding effect against incident light. The improvement in photocatalytic activity from loading of the co-catalyst depends on the balance between these two factors, producing the volcano-type dependence of photocatalytic activity.

Fig. 4 shows time courses of photocatalytic overall water splitting on the (Pt/$SrTiO_3$:Rh)–($BiVO_4$) and (Ru/$SrTiO_3$:Rh)–($BiVO_4$) systems using an Fe^{3+}/Fe^{2+} electron mediator. At the initial stage of the reaction, the amount of evolved O_2 exceeded that of H_2 on both photocatalysis systems, due to use of an Fe^{3+} salt. Fe^{2+}

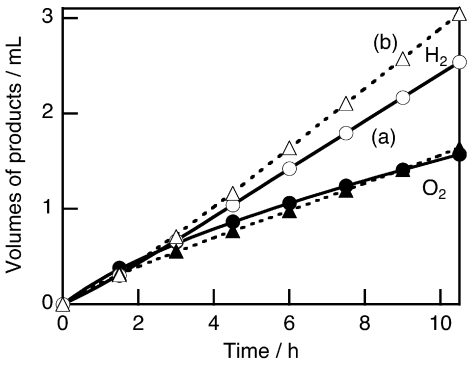

Fig. 5. Photocatalytic overall water splitting on (a) the (Ru (0.7 wt%)/$SrTiO_3$:Rh)–($BiVO_4$) system and (b) the (Pt (0.3 wt%)/$SrTiO_3$:Rh)–($BiVO_4$) under simulated sunlight irradiation. Catalyst: 50 mg each, reactant solution: 2 mmol L^{-1} of aqueous $FeCl_3$ solution, 120 mL, pH 2.4, light source: 300-W Xe-arc lamp with AM-1.5 filter, cell: top-irradiation cell, irradiated area: 33 cm^{-2}.

ions were formed by the reduction of Fe^{3+} ions on $BiVO_4$ photocatalysts, accompanied by an excess amount of O_2 when only the Fe^{3+} salt was used initially. In contrast, when an Fe^{2+} salt was used initially, similar photocatalytic activity to that achieved when using the Fe^{3+} salt was observed with an excess amount of H_2 at the initial stage. In the early stage, the system using the Pt co-catalyst had slightly higher activity than the system using the Ru co-catalyst; however, the activity of the former system decreased gradually after 10 h, and the reaction almost stopped after 50 h. This deactivation was not due to the collapse of photocatalysts, because the activity recovered after evacuation of the evolved H_2 and O_2. Rather, the deactivation seemed to be due to back-reactions accompanied by an increase in the pressures of evolved H_2 and O_2. We discuss suppression of the back-reactions in Section 3.3. In contrast to the system using the Pt co-catalyst, in the system using the Ru co-catalyst the reaction proceeded steadily for a long time even at relatively high pressure, a significant advantage. The turnover number of reacted electrons to Ru co-catalysts of 776 indicates the catalytic role of Ru. Determining the number of an active site for a photocatalyst is often difficult; therefore, the number of reacted electrons to the total number of Ru co-catalyst loaded on a $SrTiO_3$:Rh photocatalyst was used as a turnover number. The turnover number obtained by this procedure is smaller than the actual turnover number. The apparent quantum yield of the (Ru/$SrTiO_3$:Rh)–($BiVO_4$) system at 420 nm was 0.3%, similar to 0.4% of the (Pt/$SrTiO_3$:Rh)–($BiVO_4$) system.

Fig. 5 shows overall water splitting under the simulated sunlight (AM-1.5) irradiation, solar hydrogen production from water, on the (Pt/$SrTiO_3$:Rh)–($BiVO_4$) and (Ru/$SrTiO_3$:Rh)–($BiVO_4$) systems. Here the reactions were carried out in a flow system with 15 mL min^{-1} of an Ar carrier. In the system, the back-reactions were suppressed considerably, because evolved H_2 and O_2 did not accumulate in the system. With an irradiated area of 33 cm^2, the rates of H_2 and O_2 evolution were 0.30 and 0.15 mL h^{-1}, respectively, for the system using the Pt co-catalyst, and 0.24 and 0.12 mL h^{-1}, respectively, for the system using the Ru co-catalyst. The solar energy conversion efficiency of the present Z-scheme systems was about 0.02%.

3.3. Back-reactions on the system using the Ru co-catalyst

Overall water splitting in the Z-scheme system using the Ru co-catalyst proceeded steadily under the relatively high pressures of evolved H_2 and O_2 even in the closed reaction cell, as shown in Fig. 4. Under the flow condition, the deactivation was not so significant even when the Pt co-catalyst was used. These results indicate that back-reactions are suppressed in the system using the Ru co-

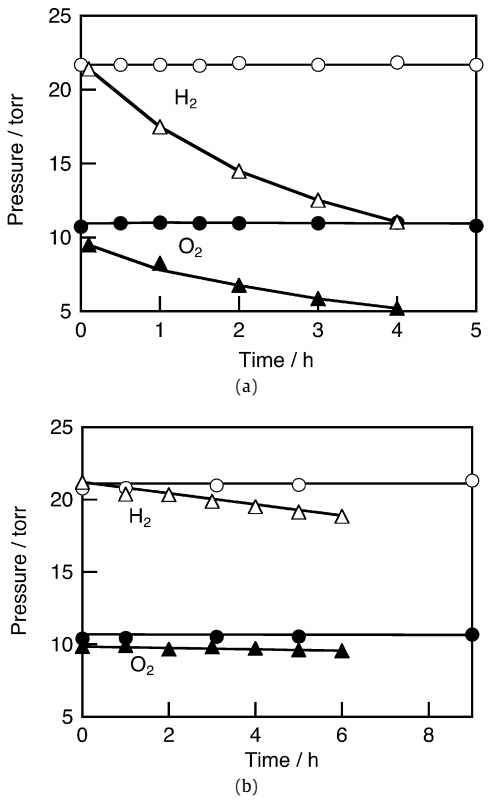

Fig. 6. Consumptions of H_2 and O_2 due to back-reactions (a) without Fe^{3+} ions and (b) with 2 mmol L^{-1} aqueous $FeCl_3$ solution on the (Pt (0.3 wt%)/$SrTiO_3$:Rh)–($BiVO_4$) (triangles) and (Ru (0.7 wt%)/$SrTiO_3$:Rh)–($BiVO_4$) (circles) systems in the dark. Open marks: H_2, closed marks: O_2. Catalyst: 50 mg each, reactant solution: 120 mL, pH 2.4 adjusted by H_2SO_4.

catalyst compared with the system using the Pt co-catalyst. The possible back-reactions are water formation from H_2 and O_2 (1), reduction of Fe^{3+} ions by H_2 (2), and oxidation of Fe^{2+} ions (3):

$$2H_2 + O_2 \rightarrow 2H_2O, \quad (1)$$

$$H_2 + 2Fe^{3+} \rightarrow 2H^+ + 2Fe^{2+}, \quad (2)$$

$$O_2 + 4Fe^{2+} + 4H^+ \rightarrow 2H_2O + 4Fe^{3+}. \quad (3)$$

Back-reactions (1) and (2) were examined with the suspension of the (Pt/$SrTiO_3$:Rh)–($BiVO_4$) and (Ru/$SrTiO_3$:Rh)–($BiVO_4$) systems in the dark, as shown in Fig. 6. After 20 Torr of H_2 and 10 Torr of O_2 were introduced into the system with the catalyst suspension, the decreases in gas pressures were monitored. Significant decreases in H_2 and O_2 pressures due to water formation were observed in the system using the Pt co-catalyst in the absence of Fe^{3+} ions (triangles in Fig. 6a). In the presence of Fe^{3+} ions, the decreases in gas pressures in the system using the Pt co-catalyst were suppressed significantly, due to the adsorption of $[Fe(H_2O)_5(SO_4)]^+$ and $[Fe(H_2O)_5(OH)]^{2+}$ ions, although slight gas consumption was still observed (triangles in Fig. 6b) [38]. The ratio of H_2 consumption to O_2 consumption was more than double, indicating reduction of Fe^{3+} ions by H_2. In contrast, H_2 and O_2 were not consumed in the system using the Ru co-catalyst in the absence and presence of Fe^{3+} ions (circles in Figs. 6a and 6b). Table 2 shows oxidation of Fe^{2+} ions by O_2 (back-reaction (3)) on the Pt and Ru co-catalysts in the dark. Oxidation proceeded on the Pt/$SrTiO_3$:Rh and Ru/$SrTiO_3$:Rh catalysts, but not on naked $SrTiO_3$:Rh; therefore, this reaction proceeded on Pt and Ru. However, the reaction rate was much faster on the Pt/$SrTiO_3$:Rh catalyst than on the Ru/$SrTiO_3$:Rh catalyst. This oxidation reaction of Fe^{2+} to Fe^{3+} with O_2 is one reason why deactivation on the Pt/$SrTiO_3$:Rh with a reaction time

Table 2
Oxidation of Fe^{2+} ions by O_2 on co-catalyst-loaded $SrTiO_3$:Rh in air at room temperature

Catalyst	Concentration of iron ions (mmol L^{-1})[a]		
	Total	Fe^{2+}	Fe^{3+}
None	1.93	1.89	0.04
$SrTiO_3$:Rh	1.84	1.77	0.07
Pt(0.3 wt%)/$SrTiO_3$:Rh	1.83	0.62	1.21
Ru(0.7 wt%)/$SrTiO_3$:Rh	1.87	1.66	0.21

[a] Reaction conditions: catalyst, 100 mg; reactant solution, an aqueous $FeCl_2$ solution; 10 mL; pH 2.4; initial concentration, 1.93 mmol L^{-1}.

was significant. Evolved O_2 can be reduced by a photogenerated electron under visible light irradiation; however, this reaction was negligible, because water splitting proceeded steadily in the presence of a certain amount of O_2, as shown in Fig. 5. These findings indicate that the Ru co-catalyst was more effective than the Pt co-catalyst in terms of suppressing back-reactions in the present Z-scheme systems using an Fe^{3+}/Fe^{2+} electron mediator.

We have reported that in the system using the Pt co-catalyst, adjusting the pH to 2.4 by adding sulfuric acid was indispensable to obtaining high activity, because $[Fe(H_2O)_5(SO_4)]^+$ and $[Fe(H_2O)_5(OH)]^{2+}$ ions covered the Pt surface under these conditions, resulting in the suppression of back-reactions [38]. But when the H_2 and O_2 pressures became high, the back-reactions were nonnegligible, resulting in deactivation. Moreover, the back-reactions proceeded when pH was adjusted to 2.4 with $HClO_4$, resulting in low activity. In contrast, in the system using the Ru co-catalyst, the back-reactions were negligible even at high pressures of evolved gases and when $HClO_4$ was used for pH adjustment. XPS measurements revealed that the surface of the Pt co-catalyst was metallic, whereas that of the Ru co-catalyst was oxidized; therefore, the back-reactions were suppressed on the Ru co-catalyst compared with the Pt co-catalyst, resulting in improved stability of photocatalytic activity.

4. Conclusion

Ru loaded on $SrTiO_3$:Rh was found to be an effective co-catalyst for overall water splitting on the Z-scheme photocatalysis system using an Fe^{3+}/Fe^{2+} electron mediator. Overall water splitting on the system using the Ru co-catalyst proceeded steadily for a long time (>70 h) even under the relatively high pressures of H_2 and O_2, whereas the activity of the system using the Pt co-catalyst decreased gradually due to back-reactions accompanied by pressure increases. Water formation from H_2 and O_2 and reduction of Fe^{3+} ions by H_2 did not proceed in the system using the Ru co-catalyst in the presence and absence of the chemical species of Fe^{3+}. In addition, oxidation of Fe^{2+} ions by O_2 on Ru co-catalyst was very slow. This is a significant advantage of the Ru co-catalyst over the Pt co-catalyst for the present Z-scheme system using an Fe^{3+}/Fe^{2+} electron mediator. Overall water splitting under a simulated sunlight (AM-1.5) on the present Z-scheme systems was experimentally confirmed.

Acknowledgments

This work was supported by Core Research for Evolutional Science and Technology program of Japan Science and Technology Agency (CREST/JST), a Grant-in-Aid (14050090) for the Priority Area Research (417) from the MEXT Japan, and the Nissan Science Foundation.

References

[1] S. Sato, J.M. White, Chem. Phys. Lett. 72 (1980) 83.
[2] J.-M. Lehn, J.-P. Sauvage, R. Ziessel, Nouv. J. Chim. 4 (1980) 623.
[3] K. Yamaguchi, S. Sato, J. Chem. Soc., Faraday Trans. 1 81 (1985) 1237.
[4] K. Domen, A. Kudo, T. Onishi, N. Kosugi, H. Kuroda, J. Phys. Chem. 90 (1986) 292.
[5] S. Tabata, N. Hirata, Y. Masaki, K. Tabata, Catal. Lett. 34 (1995) 245.
[6] A. Kudo, H. Kato, Chem. Lett. 26 (1997) 867.
[7] S. Ogura, M. Kohno, K. Saito, Y. Inoue, Phys. Chem. Chem. Phys. 1 (1999) 179.
[8] H. Arakawa, K. Sayama, Catal. Surveys Jpn. 4 (2000) 75.
[9] K. Domen, J.N. Kondo, M. Hara, T. Takata, Bull. Chem. Soc. Jpn. 73 (2000) 1307.
[10] H. Kato, K. Asakura, A. Kudo, J. Am. Chem. Soc. 125 (2003) 3082.
[11] A. Iwase, H. Kato, H. Okutomi, A. Kudo, Chem. Lett. 33 (2004) 1260.
[12] J. Sato, N. Saito, Y. Yamada, T. Takata, J.N. Kondo, M. Hara, H. Kobayashi, K. Domen, Y. Inoue, J. Am. Chem. Soc. 127 (2005) 4150.
[13] J.R. Darwent, A. Mills, J. Chem. Soc., Faraday Trans. 2 78 (1982) 359.
[14] A. Kudo, K. Omori, H. Kato, J. Am. Chem. Soc. 121 (1999) 11459.
[15] R. Konta, T. Ishii, H. Kato, A. Kudo, J. Phys. Chem. B 108 (2004) 8992.
[16] Y. Shimodaira, H. Kato, H. Kobayashi, A. Kudo, J. Phys. Chem. B 110 (2006) 17790.
[17] H. Park, W. Choi, Langmuir 22 (2006) 2906.
[18] M. Matsumura, S. Furukawa, Y. Saho, H. Tsubomura, J. Phys. Chem. 89 (1985) 1327.
[19] A. Ishikawa, T. Takata, T. Matsumura, J.N. Kondo, M. Hara, H. Kobayashi, K. Domen, J. Phys. Chem. B 108 (2004) 2637.
[20] I. Tsuji, H. Kato, A. Kudo, Angew. Chem. Int. Ed. 44 (2005) 3565.
[21] M. Hara, G. Hitoki, T. Takata, J.N. Kondo, H. Kobayashi, K. Domen, Catal. Today 78 (2003) 555.
[22] M. Liu, W. You, Z. Lei, G. Zhou, J. Yang, G. Wu, G. Ma, G. Luan, T. Takata, M. Hara, K. Domen, C. Li, Chem. Commun. (2004) 2192.
[23] K. Maeda, T. Takata, M. Hara, N. Saito, Y. Inoue, H. Kobayashi, K. Domen, J. Am. Chem. Soc. 127 (2005) 8286.
[24] K. Maeda, K. Teramura, D. Lu, T. Takata, N. Saito, Y. Inoue, K. Domen, Nature 440 (2006) 295.
[25] Y. Lee, H. Terashima, Y. Shimodaira, K. Teramura, M. Hara, H. Kobayashi, K. Domen, M. Yashima, J. Phys. Chem. C 111 (2007) 1042.
[26] T. Sakata, K. Hashimoto, T. Kawai, J. Phys. Chem. 88 (1984) 5214.
[27] G.R. Bamwenda, S. Tsubota, T. Nakamura, M. Haruta, J. Photochem. Photobiol. A 89 (1995) 177.
[28] M. Hara, C.C. Waraksa, J.T. Lean, B.A. Lewis, T.E. Mallouk, J. Phys. Chem. A 104 (2000) 5275.
[29] D. Yamashita, T. Takata, M. Hara, J.N. Kondo, K. Domen, Solid State Ionics 172 (2004) 591.
[30] I. Tsuji, H. Kato, H. Kobayashi, A. Kudo, J. Phys. Chem. B 129 (2005) 7323.
[31] A. Iwase, H. Kato, A. Kudo, Chem. Lett. 34 (2005) 946.
[32] A. Iwase, H. Kato, A. Kudo, Catal. Lett. 108 (2006) 7.
[33] K. Maeda, K. Teramura, D. Lu, T. Takata, N. Saito, Y. Inoue, K. Domen, J. Phys. Chem. B 110 (2006) 13753.
[34] K. Fujihara, T. Ohno, M. Matsumura, J. Chem. Soc., Faraday Trans. 94 (1998) 3705.
[35] K. Sayama, K. Mukasa, R. Abe, Y. Abe, H. Arakawa, Chem. Commun. (2001) 2416.
[36] R. Abe, T. Takata, H. Sugihara, K. Domen, Chem. Commun. (2005) 3829.
[37] H. Kato, M. Hori, R. Konta, Y. Shimodaira, A. Kudo, Chem. Lett. 33 (2004) 1348.
[38] H. Kato, Y. Sasaki, A. Iwase, A. Kudo, Bull. Chem. Soc. Jpn. 80 (2007) 2457.